

A Proposal to Study High Mass Photoproduction

S.D. Holmes, B.C. Knapp \*

Columbia University, New York, N.Y. 10027

D.A. Jensen, M.N. Kreisler, M.S.Z. Rabin, K. Raychaudhuri

University of Massachusetts, Amherst, Mass. 01003

J. Butler, J. Cumalat, I. Gaines, D. Harding

Fermilab, Batavia, Ill. 60510

\* Spokesperson.

Submitted September 1979

59 pgs.

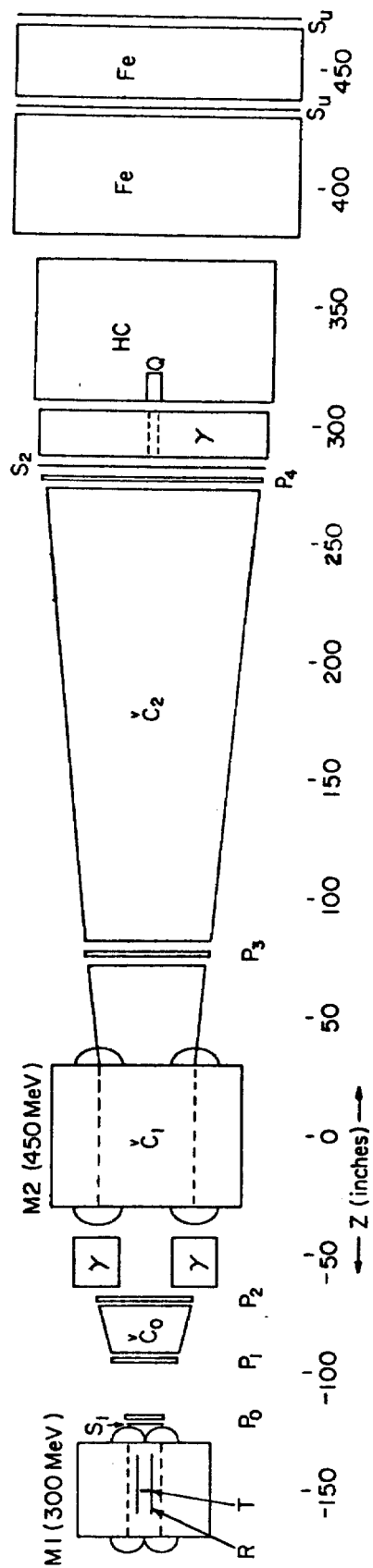


Fig. 9

## Table of Contents

	<u>Page</u>
I. Introduction	1
II. Physics Program	
A. Detection of Signals in the Presence of Backgrounds	2
B. Why Photoproduction from Nuclear Target	3
C. Isolation of Interesting High Mass Phenomena	4
III. Photon Beam	
A. Energy and Intensity Requirements	10
B. Energy Spectrum of Proposed Photon Beam	11
C. Hadron Contamination	12
IV. Detector	14
A. Detector Dimensions and Acceptance Considerations	15
B. Detector Layout	16
C. Drift Chambers	18
D. Photon Detector	19
E. Charged Particle Identification	21
F. Hardware Processor	24
V. Experiment: Interaction and Data Rates	27
A. Coherent Production	28
B. Rare Processes with Clear Signatures	30
C. Event Trigger	31
D. Comparison to Tagged Beam and $e^+e^-$ Annihilation	34
E. Future Plans	35
VI. Construction: Costs and Time Estimates	37
VII. Summary	39
References	40
Table Captions and Tables	41
Figure Captions and Figures	48

## I. Introduction

We propose an experiment in the Fermilab broad band neutral beam to study photoproduction of massive states from nuclear targets. The major physics goals of the proposed program fall into three overlapping categories:

- 1) the detailed study of diffractively produced states with masses up to  $\sim 8 \text{ GeV}/c^2$ ,
- 2) the study of photoproduced leptons pairs with masses up to  $\sim 10 \text{ GeV}$ , along with any accompanying hadrons,
- 3) the study of massive (4-12 GeV) final states with distinct signatures such as two fully reconstructed decays of massive particles with well defined masses. Included are associated production of the quantum numbers C or B and the cascade decay of a heavy particle to states containing one or more charmed particles.

To accomplish these goals requires the two essential features of the proposal, namely:

### The Fermilab Broad Band Neutral Beam

As we discuss below, the high energy and intensity available in the broad band beam make it possible to extend the mass range probed by photoproduction and to study quite rare processes.

### An Innovative Spectrometer

To observe the phenomena listed above requires a spectrometer with very high efficiency for complete and accurate reconstruction of complicated reactions at high interaction rates. While the proposed spectrometer has unusually high efficiency for reconstruction of complex multiparticle states, its most novel feature is complete on-line event reconstruction that permits the most flexible and efficient possible selection of events and also reduces off-line computation and storage requirements.

Despite the innovative aspects of the spectrometer design (or, in fact, because of them), the spectrometer is modest in cost and could be operational (i.e. taking data) within 18 months.

## II. Physics Program

As stated in the Introduction, our primary objective is the spectroscopy of heavier hadrons, particularly hadrons associated with the quantum numbers charm and bottom. We propose to achieve immediately the greatest practical detail and sensitivity by studying high energy photoproduction from nuclear targets, using a multiparticle spectrometer with unusually high reconstruction efficiency for complex states at information rates much higher than ever previously attempted. In this section, we discuss in more detail just what we wish to do and why.

### A. Detection of Signals in the Presence of Backgrounds

Our ability to observe phenomena of such general physics interest as associated production of charm is limited more by relative background levels than possible production rates. Fermilab normally produces a factor of roughly  $10^{10}$  more charm particles per hour than all existing  $e^+e^-$  colliding beam facilities, and yet the almost vanishingly low rates of the colliding beam facilities have provided almost all of our present knowledge of charm particle physics, because their background levels are so much lower than in external beam experiments.

We distinguish two types of backgrounds:

i) Backgrounds intrinsically indistinguishable from signal. If the fullest possible analysis fails to distinguish on an event-by-event basis between background and signal, one attempts at the very least to detect statistically significant departures from extrapolated backgrounds. We attempt to reduce such backgrounds by finding specific reactions or kinematic regions where signal-to-noise is maximum.

ii) Backgrounds which saturate the experimental detector at unpleasantly low signal rates. Here one encounters either the intrinsic rate limitation of the detector, such as loss

of measurement capability at detectable event rates above  $10^7$ /sec, or the rate limitation imposed by the maximum rate at which data from the detector can be digested. Counter experiments have studied specific processes with simple signatures that permit fast rejection of unwanted backgrounds by factors of  $10^2$  to  $10^9$ . Such experiments can have signal rates determined by the intrinsic rate limitation of the detector or even by the available beam intensity.

In multiparticle experiments of the type we propose, the distinction between signal and background may be quite unambiguous on an event-by-event basis but nevertheless too complicated for a traditional fast trigger decision. In Experiment 87A, for instance, we were unable to isolate candidates for charm production from much of the total cross section. We were therefore forced to keep the interaction rate low while writing 200 complex events per pulse onto tape for later off-line analysis. We believe, however, that we can now completely eliminate this limitation, by supplying sufficiently complete on-line reconstruction at the maximum rates we can envision in the broad band beam.

We describe the on-line reconstruction in more detail in Section IV. For the moment, we shall consider the technical difficulties of event selection, recording and later analysis to be adequately resolved and turn our attention to overcoming intrinsically indistinguishable backgrounds. We attempt to improve the signal-to-noise ratio at high signal rate by maximizing first the relative yield of desired reactions and second the amount of information measured for each reaction. By fully reconstructing associated production or diffractive dissociation, we both increase signal and decrease background.

#### B. Why Photoproduction from Nuclear Target

We choose photons because the photon appears to interact with less bias against new phenomena than do ordinary hadrons. Theoretically, this is because the photon couples directly to

new quarks through their electric charge.<sup>1</sup> Experimentally, charm particle production appears to be an order of magnitude larger fraction of the total hadronic cross section for photoproduction than for hadron beams.<sup>2</sup> Thus, although the absolute production cross section for charm particles is larger in hadron beams, the relative backgrounds are lower in photon-induced reactions.

We prefer a nuclear target, beryllium in particular, for much the same reason. While the total cross section per nucleon decreases slightly with increasing nuclear size, the yield per nucleon of massive states increases.<sup>3</sup> In addition, coherent diffractive production from the entire nucleus has a particularly clean experimental signature. Increasing the nuclear size much beyond beryllium is strongly inhibited by the rapid increase in the Bethe-Heitler pair production cross section.

#### C. Isolation of Interesting High Mass Phenomena

Even in photoproduction, the mere observation of high mass is not necessarily interesting. Consider the reaction

$$\gamma + p \rightarrow p + X$$

Clearly, if we see all outgoing particles we see a system whose invariant mass is just the total available center-of-mass energy. If we miss a few of the outgoing particles, we see somewhat lower mass. If we consider the invariant mass,  $M_X$ , of all outgoing particles except the proton, we expect that nearly 20% of the total cross section is diffractive dissociation of the photon, with a mass spectrum falling rapidly with increasing mass above 1 GeV. The rest of the cross section is slowly varying with  $M_X$  out to the kinematic limit. Although the majority of reactions with large  $M_X$  can be readily identified as production of two relatively low mass systems, one containing the target nucleon, it appears to us that isolation of intrinsically interesting high mass phenomena is not so simple.

Attempts to observe inclusive production of specific massive states and their subsequent decays to multihadron states suffer from large combinatorial backgrounds. Even among the final particles from a genuine charm particle pair production reaction, we would expect to find many plausible but wrong combinations of particles with invariant mass in the vicinity of a possible parent charm particle.

Thus, although in Experiment 87A we were in fact able to see single inclusive charm particle production with a small fraction of 1% of the sensitivity of the proposed experiment, we feel that our greatest sensitivity to the physics of new hadrons will lie in more highly constrained measurements, particularly fully reconstructed associated production of charm or bottom. For the production of charm and related hadrons, we expect the cleanest probe to be fully reconstructed diffractive dissociation. As we attempt to show in the remainder of the proposal, we believe that we can study the spectroscopy of these hadrons - their existence, quantum numbers, production and decay modes - with greater sensitivity and detail than any other proposed program, including  $e^+e^-$  annihilation.

### 1. Diffractive Photoproduction

By diffractive photoproduction we mean reactions

$$\gamma + A \rightarrow A + X$$

in which the nucleus remains intact and for which the resulting coherence between scattering amplitudes produces a characteristic forward peaking of the production cross section,

$$\frac{d\sigma}{dP_t^2} \propto e^{-bP_t^2},$$

where  $b$  is proportional to the square of the transverse dimensions of the nucleus. For a beryllium nucleus, the transverse momentum distribution is characterized by a slope  $b \sim 50 \text{ (GeV/c)}^{-2}$ . Thus roughly two-thirds of the



diffractive production from beryllium has transverse momentum less than 140 MeV/c. Isolation of diffractive dissociation is experimentally simple: Reject events with typically noisy nuclear breakup and require small transverse momentum.

Such a photoproduced state has the following useful properties:

i) It is produced forward with the full energy of the parent photon, thereby maximizing its detection efficiency in a forward spectrometer.

ii) It carries most of the quantum numbers of the parent photon, particularly strangeness, baryon number and helicity. We thus learn the identity, as well as the energy, of the parent beam particle.

iii) The rapidly decreasing yield of diffractively produced states with increasing mass implies small backgrounds for specific reactions.

To illustrate these features, we show in Fig. 1 the observed  $P_t^2$  distribution for exclusively produced charged pion pairs in Experiment 87A. In Fig. 2, we show the observed mass distribution for those events with  $P_t^2 < 0.05$  (GeV/c)<sup>2</sup>. We see quite clearly the coherent photoproduction of  $\rho$  and  $\rho'(1600)$ , but lose statistical significance above 2 GeV, for which we expect a thousand-fold increase in the proposed experiment. To demonstrate the utility of diffractive production, we show in Fig. 3 the inclusive pion pair mass distribution observed in the same experiment. Despite an average of almost one rho per event, the rho meson is almost invisible in inclusive multipion production, and observation of heavier states is quite hopeless.

Diffractive production can be just as useful for isolation of states other than vector mesons. Consider Fig. 4, in which we show the invariant mass distribution for the lowest mass  $\pi^+\pi^-\pi^0$  combination within coherently produced  $\pi^+\pi^+\pi^-\pi^-\pi^0$  states. A clearly visible  $\eta \rightarrow \pi^+\pi^-\pi^0$  is present with little background,

despite the fact that the decay is completely invisible in inclusive production.

Because we expect a large fraction of the yield of a massive particle to appear in diffractive production, suppression of the high mass multiparticle combinatorial backgrounds should be even more impressive for production of charm particles and their relatives. Consider, for example, our previous  $\psi$  photoproduction from beryllium or carbon nuclei. The readily identifiable  $\mu^+\mu^-$  decay permits identification of high energy  $\psi$ 's regardless of accompanying secondary particles. About half of the detected  $\psi$ 's are diffractively produced coherently from the entire nucleus. Attempts to detect hadronic decay modes would succeed readily in diffractive production, but inclusive production would be buried in background. Large fractions of accepted charm particle pairs,  $\eta_c$  and  $\chi$  states, should appear in diffractive channels such as broad resonances in the 4 to 6 GeV region.

## 2. Associated Production of Charm and Bottom

We expect to see large signals with very little background in the complete reconstruction of associated production of charm or bottom. While the relaxation of the diffractive requirement may be useful for charm production, it is essential for bottom production. As we explain in Section III, we lack sufficiently energetic photons to produce 10 or 12 GeV states coherently from the entire nucleus. But even if we divide the theoretical predictions of Ref. 1 by three, we expect roughly  $10^5$  events with an associated pair of bottom particles. Although we do not know which decay modes, if any, will be favored, we are sensitive to all decays except those including a neutrino, neutron or  $K_L$ .

We can see that associated production provides a strong rejection of backgrounds if we note that after choosing possible

decay products for one heavy particle, we have considerably fewer combinations available for the second.

### 3. Special Decay Modes of Bottom Particles

We should be able to select events containing bottom production, even if not quite fully reconstructed, by simply recording all events with a visible sum of individual particle transverse momentum magnitudes exceeding some moderately large value, perhaps 6 GeV/c. We could afford to record almost  $10^{-3}$  of the total cross section in this manner. If we produce one or more particles whose masses add up to 10 GeV or more, we would expect reasonably isotropic and relativistic decays to yield an average of at least 7 GeV for the sum of the transverse momentum magnitudes for the final decay products. This follows immediately from the observation that the average value of the sine of the polar angle is:

$$\langle \sin \theta^* \rangle = 0.785 \quad .$$

After recording most events containing bottom production, we can then search for events with only one fully reconstructed bottom particle, the other presumably missing one or more neutrals. As we discuss in Section V, we are quite sensitive to decay fractions as low as 1% to states including a  $\psi$  or one or two charm particles, even though we can readily identify only a fraction of the subsequent decays of these particles.

Note that we are expecting a signal on the order of 100 events for any reconstructable decay mode with 0.1% branching fraction. Thus we might worry more about the backgrounds than simply detectable signals. We have no reliable method for estimating backgrounds. If we consider, for example,  $B \rightarrow \psi K\pi$ , where we detect the  $\psi$  through its clear dilepton decay, we expect a mass resolution of less than 40 MeV full width. In Experiment 87A, we observed a possible continuum of 1/5 of an event per 40 MeV. If we were to scale these

events up by the same factor of 150 that we expect for genuine B decays, we would then predict 30 background events under the B signal. Whatever the purely inclusive background turns out to be, it should be further suppressed by requiring some evidence for a second bottom particle in the form of more visible transverse momentum.

#### 4. Direct or Cascade Decays to Lepton Pairs

The observation of lepton pairs,  $e^+e^-$  or  $\mu^+\mu^-$ , provides a clean experimental signature for electromagnetic coupling through a virtual photon. The most obvious example of this is the decay of heavy vector mesons. We can detect the dilepton decays of  $\psi$  or  $T$ , regardless of any accompanying particles. Both triggering efficiency and detection efficiency are nearly unity for energetic massive pairs. Backgrounds are negligible.

### III. Photon Beam

In this section, we argue that the relevant energy scale for photoproduction of a massive state varies roughly as the square of the mass being produced. We then show that the Fermilab broadband beam is by far the most intense source of high energy photons available anywhere within the next few years. We point out that for the program we propose, the hadron contamination in the beam provides negligible background and possibly some useful physics.

#### A. Energy and Intensity Requirements

For photoproduction of a state of mass  $M$ , the first and most obvious energy requirement is that the photon energy be above the threshold energy for photoproduction from a single nucleon target:

$$E_{th} = M + M^2/2M_N .$$

This is our first indication that the energy required to photoproduce a massive state varies as the square of photoproduced mass, but as we shall see this is a severe underestimate of the energies required for practical photoproduction. We consider separately the energy dependence of inclusive production of some interesting states and the energies required for coherent production from a beryllium nucleus.

#### 1. Photoproduction of $C\bar{C}$ , $B\bar{B}$ and Massive Vector Mesons

In the article by Fritzsche and Streng,<sup>1</sup> the inclusive cross sections for  $C\bar{C}$  and  $B\bar{B}$  are predicted to behave as  $(1-E_{th}/E_\gamma)$  and the exclusive cross sections for photoproduction of  $\psi$  and  $T$  from a single nucleon are predicted to behave as  $(1-E_{th}/E_\gamma)^2$  with an unphysical extrapolation to  $t = 0$ . For the vector meson photoproduction, we have chosen to provide our own fit to the experimental data for  $\psi$  photoproduction, obtaining the result shown in Fig. 5:

$$\left. \frac{d\sigma}{dt} \right|_{\theta=0} = 66 (1-E_{th}/E_\gamma)^{3.1} \text{ nb/GeV}^2 .$$

This form adequately describes the data and yields an energy dependence that scales approximately as mass squared, reaching half the asymptotic cross section at five times threshold energy.

## 2. Coherent Diffraction from Beryllium: $t_{\min}$ Effect

For coherent photoproduction from a nucleus, the minimum longitudinal momentum transfer to the nucleus is

$$q_{\min} = M^2/2E_{\gamma} \quad .$$

If the product of  $q_{\min}$  times the smaller of a coherence length or nuclear dimension becomes comparable to unity, the production is suppressed by destructive interference. Although this effect is not normally isolated experimentally from other dependence on photon energy and target recoil properties, one customarily considers coherent production to be suppressed by a factor  $e^{bt_{\min}}$ , where  $t_{\min} = -q_{\min}^2$  and  $b$  is the slope observed in transverse momentum distributions. For beryllium, a value of  $q_{\min} = 140$  MeV will suppress coherent production by a factor of three, yielding an effective threshold for coherent diffractive production:

$$\begin{aligned} E_{\min} &= \frac{M^2}{2} \sqrt{b} \\ &= \frac{M^2}{2(140 \text{ MeV})} \quad . \end{aligned}$$

In Table I, we list for various masses both the threshold energy for photoproduction from a single nucleon,  $E_{th}$ , and the effective threshold for diffractive dissociation from beryllium,  $E_{\min}$ .

## B. Energy Spectrum of Proposed Photon Beams

We now compare the two photon beams available at Fermilab and the BEG beam proposed for CERN. For both Fermilab beams we assume an incident proton intensity of  $6 \times 10^{12}$  at 400 GeV. We assume the usual 105 ft of liquid deuterium and the largest

presently available aperture for the broad band beam. To achieve highest intensity, the Fermilab tagged beam is assumed to be operated in untagged mode with a thick (20%) radiator. The CERN beam is described for 400 GeV protons and a 30% radiator. In Fig. 6, we show the photon intensity as a function of energy for these beams. For the Fermilab tagged beam we show separately the intensity for 100, 150, and 200 GeV electrons, showing the tradeoff required between energy and overall intensity. In Fig. 7, we show the number of photons above fixed energy:

$$N_{\gamma}(E_{\gamma}) = \int_{E_{\gamma}}^{E_{\max}} \frac{dN_{\gamma}}{dE} dE .$$

For energies greater than 100 GeV, the yield of photons per incident proton is a factor of ten higher for the broad band beam than for the tagged beam run in untagged mode with the relative intensities diverging rapidly with increasing energy.

The broad band beam is by far the most intense available source of photons with energies greater than 100 GeV, and with sufficient intensities between 50 and 150 GeV to require a forward spectrometer capable of very high interaction rates.

### C. Hadron Contamination

In addition to high energy photons, the broad band beam contains a small number of  $K_L$  and neutrons. Because the total cross section for hadronic interactions in the target is hundreds of times larger for  $K_L$  and neutrons than for photons, this hadron component is not negligible. We have measured the hadron contribution to the total interaction rate by simply removing the photon component with six radiation lengths of lead. We observe roughly equal contributions to the total interaction rate for energies between 50 and 150 GeV, with the hadron contribution increased to 80% of reactions between 250 and 300 GeV.

At worst, this hadron contamination of the beam might increase backgrounds by factors of two to five depending on total energy. Our emphasis on highly constrained signals should reject hadron-induced backgrounds at least as well as photon-induced backgrounds. For diffractive production, we can achieve event-by-event identification of parent particles. For more inclusive measurements such as associated bottom production, we can separate contributions to observed signals by running with and without photons in the beam. We expect hadron-induced backgrounds to be considerably reduced from the E-87A inclusive charm search, where the strange particle signature of a charm particle decay emphasized the  $K_L$  induced reactions so that 80% of the charm particle candidates were hadron induced.



#### IV. The Detector

The physics program outlined above requires a very special detector. In particular, we require:

i. A detector with very high efficiency for complete reconstruction of complex states.

ii. A detector which performs the traditional fast trigger function - selection of desired events - when the desired signature is very complicated.

iii. A detector whose performance does not deteriorate in the presence of tens of millions of detectable particles per second.

iv. A detector capable of supplying, in useful form, considerably more information than normally available for off-line study.

We will describe below a detector which meets all of these requirements. Its design has been guided in large part by our experience with the E-87A detector, whose principles of operation, strengths and weaknesses are well understood.

The new detector must have greater geometrical acceptance, more efficient particle identification and photon detection, and the ability to operate at higher interaction rates. Although the improvement in each separate item will turn out to be a modest factor, the overall increase in the product of acceptance times interaction rate will be more than a factor of 100 for those states accessible to E-87A. The largest single improvement must therefore be in the information handling, for both event selection and event recording. Although the overall improvement is a startling innovation, no new physical principles are introduced. In particular, none of the apparently sophisticated electronics involves marginal or state-of-the-art components. Even the hardware processor is built with digital circuitry (ECL 10k) which we have used for years on a comparable scale.

The modifications planned for the detector are summarized immediately below and later described in greater detail:

1. Spectrometer: We increase the solid angle acceptance by a factor of 6 over E-87A. We increase the redundancy of the wire chamber system in a manner that simplifies and improves the pattern recognition.

2. Particle identification: We greatly enhance efficiency for complete event reconstruction by increasing the segmentation and solid angle acceptance of the Cerenkov counters and photon detector, and by adding a lower threshold momentum Cerenkov counter.

3. Information handling: A preliminary design has been completed for a processor that will allow almost 100,000 events per second to be fully reconstructed on-line, with only about 10% deadtime. This will allow efficient and flexible event selection at high interaction rates. Recording the processing results will tremendously reduce off-line computation requirements.

#### A. Detector Dimensions and Acceptance Considerations

To understand the relevant dimensions of the detector, we need to consider momentarily the properties of Lorentz transformations and the spectrum of masses and energies we intend to measure. Consider a system of invariant mass  $M_X$  with laboratory energy  $E = \gamma M_X$  and velocity  $\beta \approx 1$ . In the  $M_X$  rest frame, a particle of mass  $m$  and momentum  $p^*$  is produced at an angle  $\theta^*$  away from the axis of the Lorentz transformation to the lab frame. This particle appears in the lab with an angle

$$\tan \theta_L = (1/\gamma) \frac{\sin \theta^*}{\cos \theta^* + \sqrt{1+(m/p^*)^2}} .$$

This relation is plotted in Fig. 8 for  $m/p^* = 0, 0.5, 1$ . For massive particles, the laboratory angle has a maximum of  $(p^*/m)(1/\gamma)$ . For highly relativistic center-of-mass-system particles such as photons, 80% of the center-of-mass solid angle lies within  $2/\gamma$  in the lab, 94% within  $4/\gamma$ . By

increasing the lab solid angle a factor of 4 in going from  $2/\gamma$  to  $4/\gamma$ , we pick up only 14% more center-of-mass solid angle. All K mesons with  $p^*$  less than 1 GeV appear in the lab at angles less than  $2/\gamma$ .

For photon detection we have an additional inefficiency introduced by the hole required in the photon detector for the photon beam. Here we miss a fraction of the center-of-mass solid angle  $(\gamma\theta_H)^2$ . For our present design,  $\theta_H = 5$  mr, and we lose 6% at  $\gamma = 50$ . Since more than half of the center-of-mass solid angle appears at laboratory angles less than 20 mr at  $\gamma = 50$ , the finite resolving power of the charged particle identification and the photon detector become increasingly serious problems at higher energies.

The detector described below has an inner detector that covers lab angles up to 120 mr with a highly segmented multiparticle spectrometer, and an outer detector that covers lab angles up to 250 mr with a less segmented detector designed for lower momentum particles. These angles correspond to  $2/\gamma$  and  $4/\gamma$  for  $\gamma = 16$ . We believe the detector is well designed to cover the range  $16 \leq \gamma \leq 50$  with very high efficiency for accurate reconstruction of the multiparticle states which we propose to measure.

#### B. Detector Layout

The proposed detector layout is shown in Fig. 9. The arrangement is very similar to that used in Experiments 87A and 401: two bending magnets with five stations of wire chambers, Cerenkov counters and photon/lepton/hadron detection and separation.

The target (T) is inside the first bending magnet (M1) and surrounded by a simple recoil detector (R). The narrow wire spacing drift chambers are designed to cover  $\pm 250$  mr (P0, P1, P2) and  $\pm 120$  mr (P3, P4) in both bending and nonbending views. Each chamber contains four planes, labelled x, y, u and v, measuring the nonbending view, the bending view and  $\pm 11^\circ$  away from the bending view. The individual chamber parameters are listed in Table II.

The bending magnet M2 must be a new magnet, with an aperture of 40 in. x 40 in. and a length of 60 in. The maximum desired field integral is 450 MeV corresponding to a field of 10 kG. The two magnets would normally be run with opposite polarity, with field ratios chosen to provide no net deflection 20 in. downstream of P4, permitting electrons produced in the target to pass harmlessly through the hole in the photon calorimeter. Running with opposite polarity also increases the number of desired particles transported safely through the entire spectrometer and reduces the range of angles to be covered by each mirror in the downstream Cerenkov counter. The spectrometer resolution is conservatively estimated at  $\pm 0.1$  mr, with  $\Delta p/p^2 = \pm 0.0002$  in M2 and  $\Delta p/p^2 = \pm 0.0010$  in M1. This is identical to the resolution obtained in E-87A, because we have used the improvement in spatial resolution to shorten lever arms and increase solid angle. If we succeed in achieving 100 micron rms position resolution in the drift chambers, which appears practical but unproven, our resolution will improve another factor of two.

The entire spectrometer acceptance is covered by photon calorimeter with the exception of a 4 in. x 4 in. hole for beam particles and electron pairs from the target. The region 5-120 mr is covered by a Pb/MWPC calorimeter behind the last drift chamber. This detector should have photon energy rms resolution of about  $20\%/\sqrt{E}$  and will be as finely segmented as practical, 3000 channels. The region 120-250 mr will see many fewer and lower energy particles, requiring less segmentation but better energy resolution. This region would be covered by a relatively thin Pb/MWPC and a Pb glass array, immediately in front of M2.

The Cerenkov counters C0, C1, and C2 are segmented atmospheric pressure gas counters with pion threshold momenta of 3, 6, and 12 GeV respectively. With over 200 phototubes, the segmentation and momentum range of these counters permit efficient particle identification for the range of energies,

multiplicities and masses we hope to measure.

Scintillation counter hodoscopes S1 and S2 are used in trigger formation. At the rear of the detector are a hadron calorimeter and muon identifier.

### C. Drift Chambers

The charged particle spectrometer is designed to provide high resolution and high efficiency for measurements of multiparticle states in the presence of 30 million  $e^+e^-$  pairs per pulse and 3 million muons per square meter per pulse. With 3 mm gaps between anode and cathode planes, the three upstream chambers have maximum memory times of 60 ns, and maximum drift times of 20 to 40 ns for 2 mm to 4 mm anode wire spacing. A new amplifier/discriminator recently developed at Nevis is nearly deadtimeless and has greater sensitivity than our ten year old design used in E-87A. Operating the chambers at lower gas gain and with shorter gaps than our present chambers will result in much lower stored energy and total ionization.

The drift chamber configuration is not very traditional, but is a slight variation of our present arrangement. The four planes per module include no staggered pair of parallel wires. Instead, once the track is reasonably well determined, almost any two planes form a staggered pair, so that the left/right ambiguity is resolved even when one time measurement is missing or in error. With our narrow wire spacing and wide range of track angles, the initial improvement in time and position for which wide spacing drift chambers require staggered pairs is neither necessary nor possible.

Our present experience indicates that we can reconstruct more than a dozen tracks from a single interaction in the presence of one or two unrelated photon conversions and several out-of-time hits and still have very close to 100%

reconstruction efficiency. The reconstruction algorithm was developed for Experiment 87A. We first ignore the time information and find all single view tracks which have no missing hits. Different views are then paired: two views fully determine the track, which is then fit to all planes with an iterative least square fit to five independent track parameters using the drift times and realistic magnetic field. Missing hits are thus tolerated in at most two views. With single plane inefficiencies of well under 1%, in-time tracks very seldom miss three hits.

We would use a time digitizer developed in the later stages of E-87A. It is purely digital, providing 32 time bins of width 2.5 ns, with a maximum of a single hit per wire. We have achieved finer than 200 micron resolution with the E-87A chambers which were not originally designed for time measurement. We hope to achieve 100 micron resolution, but for the purposes of this proposal we restrict our expectations to 200 microns. The individual wire plane digitizations can be read out in parallel at 10 MHz, and so an event with 10 hits per plane requires about 1  $\mu$ s for complete readout.

#### D. Photon Detector

To obtain high efficiency for full reconstruction of multiparticle states requires very high efficiency for reconstruction of a single particle in the presence of other nearby particles. We wish to build a photon detector immediately behind the last drift chamber module. This detector must be 8 ft x 8 ft with a 4 in. square beam hole. The detector must tolerate more than a million electron pairs per second produced by beam interactions in material between the two magnets. It should have sufficient segmentation and resolving power to allow separate measurement of several photons in the presence of several hadrons, with

sufficient energy and position resolution to allow identification of intermediate particles such as neutral pions and to insure accurate reconstruction of the entire event.

Since most photons result from neutral pion decay, identifying other sources of photons becomes easier if neutral pions are reliably reconstructed. Our ability to see interesting signals involving photons from other sources depends on our ability to reduce backgrounds. Identifying the two photon decay of a fairly stable particle, for instance, requires good mass resolution, but one would readily trade a factor of three in mass resolution for improved detection efficiency and a ten-fold reduction in background.

We have just completed tests of a prototype Pb/MWPC photon calorimeter which has rms energy resolution of  $24\%/\sqrt{E}$ . This is perhaps four times worse than we might be able to achieve with Pb glass counters, but is amply compensated by rms position resolution finer than 2 mm and the ability to separately resolve two showers separated by more than 4 cm.

The sampling size is set by several considerations. The spatial resolution is optimum and relatively insensitive to confusion if the shower leaves big signals in more than one element. The energy measurement is similarly insensitive to confusion if the sampling size is somewhat smaller than the shower size. The optimum would probably be a two dimensional array of  $1 \text{ cm}^2$  elements, but we see no practical way to achieve this. We plan instead to segment the detector first into quadrants, with further segmentation into 1 cm vertical and horizontal strips. The basic sample is 6 mm of atmospheric pressure isobutane with 25% argon and a trace of methylal, with electrons liberated by charged particles and then collected and multiplied by 30 micron diameter anode wires spaced 3 mm apart. Each plane of anode wires is

centered in the 6 mm gas gap between two cathode planes, one segmented into horizontal strips and the other into vertical strips. Each gas gap is preceded by a lead radiator, typically 0.5 radiation lengths, for a total of 22 radiation lengths. Corresponding strips from a sequence of gas gaps are then tied together so that their current is collected and amplified by a high gain current amplifier. The counter tested was 1 ft x 4 ft with 24 gaps, the first preceded by 1.5 radiation lengths, the next 15 preceded by 0.5 radiation lengths each and the last 8 preceded by 1 radiation length each.

The Pb/MWPC calorimeter has an output pulse width of less than 100 ns. With provision to flag out-of-time pulses, high efficiency at full resolution is possible at rates above a megacycle. We have developed a very high quality ADC compatible with the high interaction rate and high event reconstruction rate, but quite inexpensive (\$25/channel). The ADC is 12 bits, with nonlinear dynamic baseline shift. Digitization can be accomplished within 10 to 20  $\mu$ s, at the end of which time a list of pulse heights above digital pedestal is present in a separate buffer for each 256 channels. After the fast gate, the integrating capacitor can be reset within 100 ns at any time, transferred to an analog buffer within 1  $\mu$ s, or held until the output buffer is available. We have recently built 6000 such ADC's at Nevis for other experiments, but without the analog buffer and with more cumbersome readout. We require 4000 channels for this experiment.

#### E. Charged Particle Identification

Distinguishing among the charged stable hadrons ( $\pi$ , K, p) in multiparticle states is probably the most difficult challenge we presently face. The problem has received considerable attention, and possible solutions for Tevatron energies have been proposed.<sup>4</sup> We continue to rely, at least temporarily, on segmented threshold Cerenkov counters.



The disadvantages of such systems are the limited momentum range over which identification is possible and the confusion arising from finite segmentation, but they have the distinct advantage of falling within our present capabilities. We propose to improve the segmentation slightly over E-87A and to extend the momentum range to lower momenta. We postpone any serious attempt to raise the high momentum limit or achieve fully efficient segmentation.

In E-87A we used two threshold counters with pion thresholds of 6 and 12 GeV. This permitted full separation between roughly 20 and 45 GeV, with pion identification down to about 6 GeV and high energy proton identification up to about 90 GeV. We would now add a third counter with pion threshold 3 GeV, which would permit full separation down to 10 GeV and pion identification down to nearly 3 GeV.

The segmentation problem is two-fold. To eliminate confusion, not only must the number of phototubes be considerably larger than the number of particles, but the mapping of Cerenkov light onto phototubes must permit separation. If we map light from several particles uniformly over the same region, segmentation is no help. In both high threshold counters, light from a single particle illuminates a 5 in. diameter disc at the back of the counter. Viewed from the target, this is 12 mr for the downstream counter. Since the density of high energy forward particles is proportional to  $\gamma^2$ , with the entire forward hemisphere appearing at lab angles of less than  $1/\gamma$ , separation of individual particles becomes increasingly difficult at high energies.

We describe the three Cerenkov counters in Table III. We are proposing slight improvement in both the segmentation and imaging within the original solid angle acceptance of the counters C1 and C2, with much less segmentation at larger angles. In E-87A, C1 and C2 had 12 and 16 phototubes, but they covered less than 10% of the proposed solid angle acceptance and resulted in some confusion in 30% of the

accepted four-body final states.

We use rectangular arrays of spherical mirrors to reflect Cerenkov light onto phototubes. For C0 and C1, we require aluminized mylar plane mirrors to deflect the light to spherical mirrors outside the active aperture of the spectrometer. For particles from the target region with momentum above pion threshold, all Cerenkov light reaching an outer mirror is imaged directly onto the good photocathode region of a 5 in. phototube. Reflecting cones to increase the light collection of these tubes would only increase the number of undesirable photons from other sources. Each inner mirror focuses Cerenkov light onto a rectangular mirror baffle which further segments the light with at most one grazing reflection onto small (1.6 in.) phototubes.

If the segmentation were fine enough, and in the focal plane of each spherical mirror, we could measure the Cerenkov angle. With considerably coarser segmentation than would be required for a true imaging counter, we instead attempt to minimize the spread of light from a single particle compared to particle separations. We therefore focus on each baffle a sharp image of the center plane of the Cerenkov counter.

The total number of phototubes is modest: twenty-four 5 in. tubes and one-hundred and eighty 1.6 in. tubes. The small tubes are only ten stage and require fast amplifiers with small dynamic range but rapid recovery from overload. These small tubes are expected to cope with the light from the 30 million electron pairs per pulse. Our experience has also shown that the tubes must cope with modest rates of charged particles passing through their glass envelopes, producing quite large signals.

#### F. Hardware Processor

The experimental program outlined in this proposal requires fairly complete on-line event reconstruction within tens of microseconds. Since the Fermilab Cyber 175 system takes a thousand times longer to perform the same computation, this might at first glance appear to be a difficult and dangerous requirement. We believe, however, that such information processing power has been possible for the past few years, using simple, reliable and inexpensive processors assembled for specific problems.

We first develop a general approach to such processing by identifying small simple hardware elements and simple rules for their interconnection that permit any digital computation to be performed with optimum efficiency, measured in operations/second/dollar. Such a general approach not only permits general application, but is probably necessary for practical solution to a specific complex problem which probably spans most of the general features of digital computation by itself.

Our understanding of the general principles continues to evolve. Had we built the proposed processor a year ago, it would have worked exactly as expected. Today we can build a smaller version that would be twice as fast. After building and using such a device, we could undoubtedly do even better, but the original device would remain functional and compatible with any expansion of the problem.

The general principles are quite simple. Data are transferred from register to register under control of a central clock. The clock period, presently 25 ns, is determined by the time required for register to register transmission through an intermediate arithmetic operation, memory reference or intermodule transmission line. Central control is exerted only by the clock, and by a control/communication bus which is idle during normal processing, but can be used to access any register in the system from the outside, allowing diagnostic exercises and the loading

of tables.

In general, we have neither central memory nor stored program. Memory is an integral part of the processor, providing tables of precomputations, lists of variable data, and maps. Three essential control functions appear in the computation data paths:

- i. V, here is a new data element (from source).
- ii. C, sequence of data elements is complete (from source).
- iii. H, unable to accept transmission (from receiver).

A computation requiring  $n$  sequential steps can be performed in a pipeline of  $n$  distinct hardware elements so that the delay through the pipeline is  $n$  cycles, but a new computation can begin each cycle. Many such pipelines can operate simultaneously and independently. Such a structure is called a pipelined parallel processor.

The parallel pipeline structure appears at more than one level. On a macroscopic scale we expect an event to have analog signals digitized in parallel with track reconstruction, while at the same time the previously accepted event is undergoing kinematic reconstruction. Such a pipeline may eventually be several events deep. All information that might eventually be used must be stored until the final disposition decision.

Additional, possibly unforeseen, computations can always be added, either in parallel at some stage of the pipeline, or in series as a new pipeline stage. Such new computations should not affect the rate of event reconstruction.

The incredible cost effectiveness of computation in this structure results from the possibility of using simple special purpose devices for their specific purposes at full speed with few idle periods. The pipeline structure almost guarantees this capability. Operations which must be performed very many times can be unfolded into a large fast pipeline, while infrequently performed operations can be folded in several ways to maintain the same operations/second/dollar.

The processor can be simulated exactly in Fortran on a normal computer so that one can study the processor performance before actually building it. We construct software modules that simulate corresponding hardware modules exactly, and then specify their interconnections, including the control/communication bus. Given the input data for the computation, we can predict the status of every element in the processor, cycle by cycle. We thus determine how long the computation would require and what the result would be. We thus isolate bottlenecks and underutilized hardware. Both the hardware and the software version can analyze raw data from tape. In addition to the necessary diagnostic and developmental studies, this permits use of the processor for Monte Carlo studies.

We have preliminary designs for a data analysis, selection and histogram structure which would permit studies of very high rate processes without recording individual events on tape. We do not anticipate such rates for reactions of general physics interest in the proposed experiment, nor do we see clearly how to make use of such rates yet, but such a feature will allow on-line diagnostic and calibration studies continuously without interfering with the selection and recording of events of more general physics interest.

The size, physical complexity, and cost of the processor are all small compared to the hardware supplying the input data. The design and construction of actual hardware should always be quick and simple. The time and complexity appear at the software level.

# V. The Experiment: Interaction and Data Rates

We anticipate running with  $3-6 \times 10^{12}$  400 GeV protons per pulse incident on the existing beryllium target. The neutral beam collimators would be set at the present maximum aperture with the 32 m of liquid deuterium in place. The experimental target would be a piece of beryllium 1.75 cm thick (5% radiation length), in which about 4% of photons and 5% of hadrons interact. On the average, secondary particles have about 2.5% probability of interacting, and so about 10% of the four-body final states suffer secondary interactions within the target.

We have designed a detector which should perform well at the very high rates accompanying  $6 \times 10^{12}$  protons per pulse and the largest beam size. Such high intensity may not always be available or desirable, but will be assumed for consideration of the instantaneous rates and the challenge they present. Total integrated rates are based on an exposure of about  $10^{18}$  protons, which would be 500 hours at  $6 \times 10^{12}$  or 1000 hours at  $3 \times 10^{12}$ , assuming 400 pulses per hour. For such a run, the integrated luminosity is  $3.7 \times 10^4/\text{nb}$  for photons above 50 GeV, and  $1.4 \times 10^4/\text{nb}$  for photons above 100 GeV. The integrated luminosity in E-87A for energies above 50 GeV was  $1.0 \times 10^3/\text{nb}$ .

At  $6 \times 10^{12}$  incident protons and the largest collimator setting, the neutral beam at the photon target provides about  $10^8$  photons with energy above 50 GeV within a spot size 7 cm x 7 cm. Extrapolating from Experiment 87A, the total rate of  $e^+e^-$  pair production in the target will then be  $3 \times 10^7$  pairs/pulse, and the peak muon flux in the area will be less than  $3 \times 10^6/\text{meter}^2/\text{pulse}$  or about 15 million muons per pulse incident on the entire detector. The total rate of hadron production by photons with energy above 50 GeV is more than  $2 \times 10^4$  per pulse, with a similar number produced by energetic hadrons in the beam and about twice as many produced by lower energy photons. We summarize these running conditions in Table IV.

We summarize below the acceptance and expected rates for selected states based on extrapolations from rates observed in E-87A or on current theoretical predictions. States are divided into two overlapping categories: those that we expect to observe in coherent diffraction from the entire nucleus and those representing interesting rare events with sufficiently clean signatures that we would not require coherent production to isolate the signal from backgrounds.

We expect an increase in observed signal over E-87A that depends on the state in question, but ranges dramatically upward from a factor of more than 200. There are several factors responsible for this increase. The total luminosity is a factor of 37 higher. In general, the geometrical acceptance has increased by at least a factor of 4, and the triggering efficiency by at least a factor of 2. The probability of unambiguous identification of a typical charged hadron has increased from less than 0.7 to more than 0.9, and the possibility of efficient detection of photons in multi-particle final states becomes at last possible. This enormous increase in the efficiency of identification of charged particles and the detection of photons permits not only a large increase in signal but also a large reduction of backgrounds.

#### A. Coherent Production

In Table V, we list acceptance and expected rate for a representative sample of coherently produced final states. We have not included odd pion final states, or in fact any final states containing photons, because of the difficulty of extrapolating from E-87A. We plan to study such states and expect a majority of states with more than two charged particles to contain photons. Many interesting states for which our detection efficiency is high have no reliable estimates for production cross sections, but should be readily visible. Such states include high mass vector mesons and diffractively produced continuum which decay into charm-anticharm pairs or states containing  $\eta_c$ 's or  $\chi$ 's.

We see from Table v that not only do we expect large numbers of events at high masses, but we have extremely large samples at masses below 3 GeV. We now consider the listed states:

1.,2.) The coherent  $\pi^+\pi^-$  mass distribution from E-87A has already been shown in Fig. 2. The figure shows  $\rho$  and  $\rho'$  along with some possible structure near 2.1 GeV. This distribution should become more interesting with the increase in statistics by a factor of 1000 which we anticipate for masses above the  $\rho$ .

3.) The large number of events expected in the four charged pion channel will allow a thorough study of the still puzzling decays of the  $\rho'(1600)$ . Comparable statistics can be expected for the  $\pi^+\pi^-\pi^0\pi^0$  state. Any higher mass structures should be observable up to masses of about 8 GeV, and should become easier to understand when widths are small compared to the difference from threshold mass.

4.,5.)  $K^+K^+K^-K^-$  or  $K^+K^-\pi^+\pi^-$ : As in the four pion state, information will be available out to about 8 GeV with very high statistics at lower masses. One intriguing possibility is the existence of  $\phi\phi$  resonances. The three  $\phi\phi$  events observed in E-87A all lie within 50 MeV of 2.4 GeV. Our sensitivity to this state is about 30 events/pb. Our ability to see Primakoff production of  $\eta_c$  will depend on the branching fraction of  $\eta_c$  into the specific channels such as  $\phi\phi$  and the partial width into  $\gamma\gamma$ . According to Quigg and Rosner,<sup>5</sup> the Primakoff cross section at 200 GeV is,

$$\sigma(\gamma + \text{Be} \rightarrow \eta_c + \text{Be}) = (10 \text{ pb/nucleon}) \frac{\Gamma(\eta_c \rightarrow \gamma\gamma)}{1 \text{ keV}}.$$

Irrespective of whether we see Primakoff production of  $\eta_c$  we do expect to see  $\eta_c$  in coherent production with additional hadrons, just as we see copious production of  $\pi^+\pi^-$ .



### B. Rare Processes with Clear Signatures

In Table VI, we list acceptance and predicted event rates for specific rare processes. We leave out examples of conventional particle production that could be selected, such as  $\Lambda\bar{\Lambda}$  and  $\Omega\bar{\Omega}$ . We now discuss some of these processes in detail:

2) In E-87A we observed 90 events containing a  $\psi$  plus hadron, of which 30 events contained at least one identified K meson. Extrapolating from this we would expect to see 250 times as many  $\psi$  accompanied by hadrons, and provide more complete measurement of the hadrons. This implies 13,000 such events with 4,000 containing an identified K meson. These events are interesting for several reasons other than simply studying properties of inclusive  $\psi$  production. Observation of the accompanying particles should provide information about the dynamics of charm production, including illumination of OZI predictions. Other possibilities include the observation of heavier states which decay to  $\psi$  plus other particles, whether by weak, electromagnetic or strong interaction.

3) As shown in the table, we expect more than a million events with a fully reconstructed D meson. Inclusive D meson production in itself is probably not best done in this experiment, but triggering on a visible D candidate would allow us to look for associated production of other charm particles or decays from a higher mass narrow state. Specific known decay modes of the  $\Lambda_c$  are equally easy to select. Cross sections for production of other states in association with observable known decays are not known, but production of F mesons and the remaining baryons will be observable unless suppressed by two orders of magnitude relative to  $D\bar{D}$ .

4) Bottom production: The model of  $B\bar{B}$  production discussed in Ref. 1 predicts an asymptotic cross section for  $B\bar{B}$  production of 27 nb, with an energy dependence similar to

that given in Fig. 5. The model is quite simple and predicts cross sections for photoproduction of heavy quarks which scale to lowest order as  $\sigma \propto (e_q/m_q)^2$ . The model predicts an asymptotic charm cross section of about  $1.0 \mu\text{b}$  and a  $\psi$  cross section of  $50 \text{ nb}$ . In E-87A we measured

$$\sigma(\gamma + C \rightarrow D^0 + X) \approx 500 \text{ nb/nucleon}$$

$$\sigma(\gamma + C \rightarrow \psi + X) \approx 30 \text{ nb/nucleon}.$$

Integrating the predicted energy dependent cross section over the photon spectrum, we obtain a total of  $325\text{K}$   $B\bar{B}$  events, most of which should be fully within our acceptance. The fraction of these decays which can be reconstructed is unknown, of course. We cannot reconstruct states with a neutrino, a neutron or a  $K_L$ . Even with a wide range of detectable decay modes, we should be able to see  $B\bar{B}$  production by requiring fully reconstructed associated production. Specific cascade decays to  $\psi$  and charm particles may permit observation of single B inclusive production.

5) Our estimated upsilon production is based on a related prediction for the cross section, which becomes  $270 \text{ pb}$  at high energies. Using the energy dependence which we obtained for the  $\psi$ , and assuming a leptonic branching ratio of  $4\%$ , we predict  $30$  detected  $T \rightarrow l^+ l^-$ .

### C. Event Trigger

We propose to record any event falling into one of the following three categories:

1) Any coherently produced state, except low mass pion pairs, with energy above  $50 \text{ GeV}$ . Experimentally, coherent means total observed charge zero, low  $P_t^2$  and nothing detected in a recoil detector sensitive to fairly low energy photons. Since coherent diffractive photoproduction represents about  $5\%$  of the total cross section, with the  $\rho$  excluded, this would be well over a thousand events per pulse, including hadron induced events. Because we have no desire to fill a

magnetic tape every 5 minutes, the majority of these events would be recorded in very compact form, averaging about twenty 16-bit words per event. Rare and unusually interesting events would be recorded in greater detail, including raw drift chamber data and/or raw ADC data (no pedestals). If unnecessarily large numbers of low mass events would be recorded this way, we could always choose to record a fixed fraction of the low mass and low multiplicity events.

2) Any state containing a lepton pair, except low mass Bethe-Heitler. Even including low mass Drell-Yan and vector meson decays, this amounts to less than  $10^{-3}$  of the total cross section.

3) Candidates for clear signature production of C or B. This would include candidates for specific charm particle decays with enough visible mass to be candidates for reconstructed associated production or cascade from a heavier state. The charm particle decay must be to fully identified hadrons and have a mass within experimental resolution ( $\leq 5$  MeV) of the correct mass. To also include most  $B\bar{B}$  production but keep the number of candidates below  $10^{-3}$  of the total cross section, we would record events with at least 6 GeV for the sum of the individual particles' transverse momentum (magnitude).

We hope to write less than half as many words per pulse onto tape as in E-87A, or at most 32 K 16-bit words per pulse, composed roughly equally of 500-800 low mass simple topologies recorded in compact form and 50-80 fully recorded complex or rare events. In 500 hours of 400 pulses each, for a total of  $2 \times 10^5$  pulses, this translates to more than 10 million rare events and 100 million simple topologies, carefully selected with full off-line precision from  $4 \times 10^9$  high energy photo-production reactions and a comparable number of neutron and  $K_L$  induced reactions.

We envision a triggering scheme similar at the primitive level to the one used in E-87A. We first form a fast trigger (Master Gate) which is used to gate ADC's, TDC's and coincidence registers. The decision to accept the event for the next stage of processing, that is track reconstruction and charge digitization, is formed by a slow trigger (DC logic) which performs nonrecursive digital operations based on the status of drift chamber TDC latches and of coincidence registers which record scintillation counter coincidences and low precision (1 to 4 bits) analog-to-digital conversion. The gate widths, the DC logic time and the time required to reset the ADC's are each nearly 100 ns. The Master Gate deadtime is therefore about 250 ns and so the Master Gate rate must be kept below 400 kc to keep its contribution to total system deadtime below 10%. This is considerably less than the 30 million electron pairs produced in the target or the 15 million random muons at the back of the detector, but ten times the number of energetic hadronic final states produced in the target each pulse.

The Master Gate is therefore to be the sum of two unrelated triggers: the first attempting to pick up all target interactions except muon pairs and low mass Bethe-Heitler electron pairs by requiring a minimum of perhaps 5 GeV in calorimeters that fill the aperture except for the beam hole and that portion of the photon calorimeter accessible to low mass electron pairs produced by beam interactions with material between the two magnets. The second trigger attempts to pick out muon pairs coming from the target region by using scintillation counter hodoscopes in the nonbending view. This suppresses the few million random coincidences per pulse between muons illuminating the largest areas of the detector without passing near the target region. We anticipate no difficulty in keeping the Master Gate well below 400 kc.

The slow trigger must then reduce the trigger rate to the level of 50 kc. This can be done with a sum of simple triggers requiring something more impressive in the calorimeters or using the drift chambers as fine grained hodoscopes to guarantee charged particles from the target vicinity other than low mass electron pairs.

Upon a slow trigger decision to analyze further, about a microsecond is then required to transfer all the analog and digital information to processing buffers before the detector is ready to accept another event. We can therefore operate with a total deadtime of 250 ns times the Master Gate rate plus about 1  $\mu$ s times the slow trigger rate for a total of 10% to 20% deadtime, even though we require 10 to 20  $\mu$ s to analyze each of more than 50 K events per second.

#### D. Comparison to Tagged Beam and $e^+e^-$ Annihilation

We regard the program set forward in this proposal as complementary to the program planned in the tagged photon laboratory. Although there will inevitably be some overlap in the physics produced we intend to concentrate our efforts on those areas which are dependent upon the high energy and high intensity of the broad band beam. In our view, there are two such areas:

1. Photoproduction of very high mass states. We have argued that the production of states with masses in the range  $5-12 \text{ GeV}/c^2$  is best accomplished in the broad band beam owing to its relatively high intensity at high energy.

2. Photoproduction of rare events with complicated topologies. We have argued that the observation of rare events with complicated but well defined signatures is possible only if running is done at very high intensities with a detector capable of correctly identifying and measuring such events.

We would not expect to compete with the tagged beam in areas in which a knowledge of the photon energy or the

lack of hadron contamination in the beam is critical. (Such an area would be measurement of the energy dependence of inclusive charm production.) However we do expect to be able to study final states such as very high mass vector mesons, associated production of charm pairs with each particle decaying through an observable decay mode, and the inclusive production of B mesons which are beyond the reach of the tagged beam due to the two considerations listed above.

Most of the states accessible to photoproduction experiments can also be observed in  $e^+e^-$  interactions. However, there are major differences, the main one being that the entire mass range is covered simultaneously in photoproduction. In general, rates (measured in events/hour) for the production of specific vector mesons are higher in storage rings run at the appropriate energies, while rates for charmed particle production (and presumably B meson production also) are orders of magnitude higher in photoproduction. For example, in  $e^+e^-$  annihilation at the 3.77 GeV resonance, the  $D^0\bar{D}^0$  cross section is  $\sim 10$  nb ( $\sim 2$  nb off resonance) while in photoproduction the cross section is  $\sim 500$  nb. The time averaged luminosity for the experiment proposed here is  $2.1 \times 10^{31}/\text{cm}^2/\text{sec}$  (assuming 1 pulse every 9 sec) which is comparable to the luminosity obtainable in  $e^+e^-$  storage rings.

#### E. Future Plans

We hope eventually to extend the experimental program of this detector to hadron induced reactions and to the higher masses and energies which become accessible with TeV protons. The present broad band beam can readily become a high quality neutron or  $K_L$  beam. Both the detector and the present beam line are compatible with the efficient utilization of whatever proton beam is available during the possibly hectic transition to a superconducting main ring of energy up to 500 GeV.

Because the laboratory angles of secondary particles decrease with increasing energy, practical secondary beams can be built with considerably higher intensities, as well as higher energies. Several members of this collaboration

are presently involved in the design of a high energy  $e/\gamma$ /hadron beam line which would be available after the Proton Lab is upgraded to Tevatron energies. Operated as a broad band photon beam, it would have high intensity of higher energy photons with no hadron contamination. Charged or neutral hadron beams would also be available.

We have designed the presently proposed detector so that the changes required for operation in the Tevatron beam would consist of additions to the proposed detector without replacement of any major elements. The longitudinal dimensions of the detector would increase, but not the transverse dimensions.

To take full advantage of the Tevatron beam would require two major advances in the detector operation, which we believe we could make after the program of the present proposal is well underway. The only real hardware challenge is the extension of charged hadron identification to higher energies. At the moment, we suspect that this could be accomplished by converting the inner segments of C2 to high precision imaging Cerenkov counter, using highly segmented phototubes with micro channel dynode structures. The other advance which we believe possible, but do not wish to explain or defend at this point, is the efficient utilization of the two or three orders of magnitude increase in information rate possible in hadron beams. Interaction rates of more than  $10^6$  high energy hadrons per second are possible and should be compared with more like  $10^4$  for high energy photons in this proposal.

# VI. Construction: Costs and Time Estimates

We estimate construction costs for new equipment plus replacement cost of old equipment which we wish to use to be:

	<u>Mechanical</u>	<u>New Electronics</u>	<u>Old Electronics</u>	<u>Total</u>
Drift Chambers	\$ 90 K	\$110 K	\$ 40 K	\$240 K
Hardware Processor		100 K		100 K
Photon Calorimeter	100 K	160 K		260 K
Cerenkov Counters	100 K	40 K	40 K	180 K
Hadron Calorimeter	45 K	15 K		60 K
Muon Identifier	10 K	10 K	20 K	40 K
Trigger and Recoil System	10 K	10 K		20 K
	<u>\$355 K</u>	<u>\$445 K</u>	<u>\$100 K</u>	<u>\$900 K</u>

We request a major piece of new equipment from Fermilab: an analyzing magnet with one meter square useful aperture, providing a field integral of 15 kG meter with a pole length of at most 1.5 meters. We also request that the lab supply material for the muon identifier.

The \$45 K mechanical assembly cost of the hadron calorimeter includes an estimate of the cost of replacing the existing 5 ft x 6½ ft iron plates with 9 ft x 9 ft iron plates. We could make use of much of the E-87A cabling, MWPC electronics, phototubes, and scintillator for a total of at least \$100 K of the estimated \$900 K of new equipment.

All electronics, the drift chambers, Cerenkov counters, hadron calorimeter and muon identifier could be installed within 12 months of approval and funding. Construction and installation of a new analyzing magnet and photon calorimeter



might require 18 months. With installation of the drift chamber system and track reconstruction hardware, we would wish to use muons accompanying targeting for the Tagged Photon Facility (TPF) for debugging and calibration. If approved in November 1979, we could be fully operational by mid-1981 without disturbing any other experimental program.

Predictions of long mid-year accelerator shutdown for construction, present uncertainties associated with transition to superconducting main-ring operation, and the prospect of proton lab "pause" for upgrading to Tevatron energies, all make predictions of running schedules difficult. We could be ready by mid-1981, installed in the present 87-A pit EE4. Operation of the present broad band beam with the detector in EE4 is compatible with construction of a new beam line. The present beam and detector location would not be compatible with TPF operation, but our proposed physics program requires sufficiently modest running time, about 10 calendar weeks, that interference with the tagged beam program should be minimal. We would hope later to move the detector into a new proton beam line which would permit utilization of TeV protons simultaneously with TPF operation.

We believe that our off line computation requirements will be less than those of E-87A. We wish to retain the Fermilab PDP-11 presently used for data acquisition.

## VII. Summary

We have discussed in this proposal a program to study the photoproduction of high mass hadronic states. We believe that the exciting physics contained in these states is best extracted through the wide band neutral beam used in conjunction with the proposed detector. The experiment as described can be mounted for a modest cost over a reasonable time period, and has been designed to have a natural extension to the Tevatron.

# References

- 1 H. Fritzsch, K.H. Streng, Phys. Lett. 72B, 385 (1978).  
B. Margolis, Phys. Rev. D17, 1310 (1978).  
H. Fritzsch, K.H. Streng, Phys. Lett. 78B, 447 (1978).
- 2 M. Atiya et al, Phys. Rev. Lett. 43, 414 (1979).  
K.W. Brown et al, Phys. Rev. Lett. 43, 410 (1979).
- 3 The study of dilepton and dihadron production at high mass  
and single (inclusive) hadron production at large  $P_T$   
indicates that the A dependence of these processes is  
characterized by  $A^\alpha$  where  $\alpha$  is typically 1.1-1.2, while  
for the total hadron-hadron cross section  $\alpha$  is typically  
0.8. The A dependence of the total photoproduction cross  
section is given by  $\alpha \approx 0.9$  while the high mass photo-  
production is unmeasured. See,  
J.W. Cronin et al, Phys. Rev. D11, 3105 (1975).  
R.L. McCarthy et al, Phys. Rev. Lett. 40, 213 (1978).  
D.M. Kaplan et al, Phys. Rev. Lett. 40, 435 (1978).  
K.J. Anderson et al, Phys. Rev. Lett. 42, 944 (1979).  
R.M. Egloff, Ph.D. Thesis, University of Toronto (1979).
- 4 W. Willis, Physics Today, October, 1978.
- 5 C. Quigg, J.L. Rosner, Phys. Rev. D16, 1491 (1978).

### Table Captions

- I. A compilation of  $E_{\min}$  and  $E_{\text{th}}$  as a function of mass  $M$ .  
 $E_{\min}$  is the photon energy needed to produce a  $t$  value of  $0.02 \text{ GeV}^2$  while  $E_{\text{th}}$  is the production threshold energy.
- II. Wire chamber sizes and wire spacings.
- III. Cerenkov counter design parameters.
- IV. A summary of the proposed running conditions.
- V. Rates for selected coherent processes.
- VI. Rates for selected rare processes.

Table I

$M(\text{GeV})$	$E_{\min} = M^2/2(0.14)$	$E_{\text{th}} = M + M^2/2M_N$
1	3.6	1.5
2	14.3	4.1
3	32.1	7.8
4	57.1	12.5
5	89.3	18.3
6	129.	25.2
7	175.	33.1
8	229.	42.1
9	289.	52.2
10	357.	63.3
12	514.	88.8

Table II

<u>Chamber</u>	<u>Distance From Target</u>	<u>Dimension</u>	<u>Spacing</u>	<u># of Wires</u>
P0 X Y, U, V	30 in.	15" x 15"	2 mm	192 192 x 3
P1 X Y, U, V	55 "	30" x 30"	3 mm	256 256 x 3
P2 X Y, U, V	80 "	40" x 40"	4 mm	256 256 x 3
P3 X Y, U, V	226 "	53" x 68"	6 mm	224 288 x 3
P4 X Y, U, V	430 "	91" x 113"	6 mm	384 480 x 3
				5728 wires

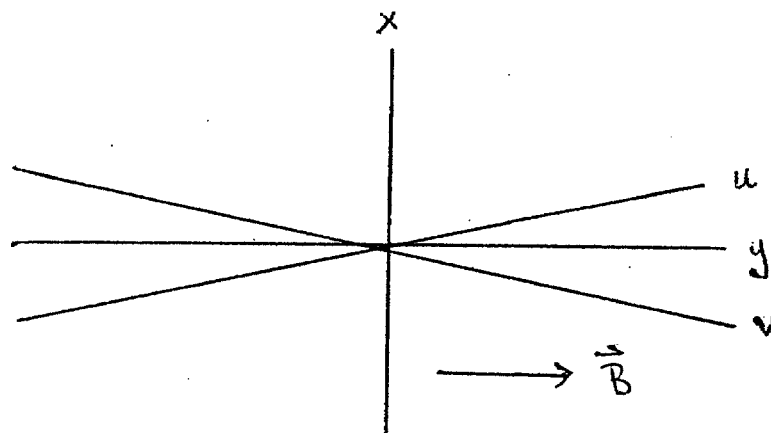


Table III

Cerenkov Counter

	<u>C<sub>0</sub></u>	<u>C<sub>1</sub></u>	<u>C<sub>2</sub></u>
Radiator	C <sub>4</sub> H <sub>10</sub>	N <sub>2</sub>	N <sub>2</sub> /He
(n-1)x10 <sup>6</sup>	1200	300	75
Pion Threshold	3	6	12
Length	20 in.	100 in.	180 in.
Downstream Size	40 " x 40"	48" x 48"	100" x 100"
Number of Spherical Mirrors	16	20	25
Size of Mirrors	12" x 12"	16" x 16"	20" x 20"
$\theta_c$	50 mr	25 mr	12 mr
# of Photoelectrons	6	8	4

Segmentation

C<sub>0</sub>


1	6	6	1
1	6	6	1
1	6	6	1
1	6	6	1

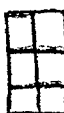
C<sub>1</sub>


1	4	4	1
1	<del>6</del>	<del>6</del>	1
1	<del>12</del>	<del>12</del>	1
1	<del>6</del>	<del>6</del>	1
1	4	4	1

C<sub>2</sub>

1	1	4	1	1
1	<del>4</del>	<del>6</del>	<del>4</del>	1
1	<del>6</del>	12	<del>6</del>	1
1	<del>4</del>	<del>6</del>	<del>4</del>	1
1	1	4	1	1

4 = 

6 = 

12 = 

Note: Dotted lines correspond to E-87A acceptance.

Table IV

Conditions:  $6 \times 10^{12}$  ppp at 400 GeV, Large hole in CF408B  
CF410B,  
32 m of D<sub>2</sub> .

Target: 5% r.l. of Be  
e<sup>+</sup>e<sup>-</sup> rate =  $30 \times 10^6$ /pulse  
 $\mu$ 's =  $3 \times 10^6$ /m<sup>2</sup>/pulse  
L =  $18.5 \times 10^{-2}$ /nb/pulse ( $E_\gamma > 50$  GeV)  
Hadronic Rate = 22,000/pulse  $E_\gamma > 50$   
8,400/pulse  $E_\gamma > 100$

For  $2 \times 10^5$  pulses (500 hours)  
L =  $3.7 \times 10^4$ /nb  $E_\gamma > 50$  GeV  
 $1.4 \times 10^4$ /nb  $E_\gamma > 100$  GeV  
 $5.1 \times 10^3$ /nb  $E_\gamma > 150$  GeV



Table V  
(Coherent Processes)

<u>State</u>	<u>E87 (Obs)</u>	<u>Acc.87</u>	<u>Acc New</u>	<u>Expected</u>
1. $\gamma \rightarrow \rho' (1600) \rightarrow \pi^+ \pi^-$	800	0.04	1.00	720 K
2. $\gamma \rightarrow \pi^+ \pi^- > 1 \text{ GeV}$	7500	0.04	1.00	6.7 M
$> 2$	400			360 K
$> 3$	50			45 K
3. $\gamma \rightarrow 4\pi > 1 \text{ GeV}$	60,000	0.15	0.98	14 M
$> 2$	11,000			2.6 M
$> 3$	1100			260 K
$> 4$	100			24 K
$> 5$	10			2.4 K
4. $\gamma \rightarrow K^+ K^- K^+ K^- > 2 \text{ GeV}$	50	0.05	0.40	14 K
$> 3$	8			2.3 K
$> 4$	1			300
$\phi\phi$	3			860
5. $\gamma \rightarrow KK\pi\pi > 1 \text{ GeV}$	7000	0.09	0.75	2.1 M
$> 2$	5000			1.5 M
$> 3$	500			150 K
$> 4$	70			21 K
$> 5$	10			3 K

Table VI  
(Rare Processes)

<u>State</u>	<u>E87 (Obs)</u>	<u>Acc 87A</u>	<u>Acc New</u>	<u>Expected</u>
1. $\gamma \rightarrow \psi$				1.1 M
$\mu^+ \mu^-$	350	0.15	0.97	80 K
$e^+ e^-$	100	0.05		80 K
2. $\gamma \rightarrow \psi + \text{hadrons}$	90	0.20	0.80	13 K
$\psi + K + \text{hadrons}$	30	0.15	0.52 *	3.7K
$\psi' \rightarrow \psi \pi \pi$	15	0.20	0.85	2.3K
$\hookrightarrow \mu^+ \mu^-$				
3. $\gamma \rightarrow D^0 (\bar{D}^0) + \text{any } (\sigma = 500 \text{ nb})$				18 M
$\hookrightarrow K^+ \pi^-$	100	(0.005)	0.57 *	400K
$\hookrightarrow K^+ \pi^- K^- \pi^+$	(1)	(0.005)	0.45 *	3.2K
$\hookrightarrow K^+ \pi^- K^- \pi^+ \pi^- \pi^+$	(4)	(0.01)	0.46 *	6.6K
4. $\gamma \rightarrow B(\bar{B}) + \text{any } (\sigma = 27 (1 - \frac{E_{th}}{E}) \text{ nb})$				325K
$\hookrightarrow \psi K^+ \pi^- \rightarrow \ell^+ \ell^- K^+ \pi^-$			0.60 *	550 (1% BR)
$\hookrightarrow D^0 \pi^\pm \rightarrow K^\pm \pi^\mp \pi^\pm$			0.50 *	85 (1% BR)
5. $\gamma \rightarrow T \quad (\sigma = 270 (1 - \frac{E_{th}}{E})^3 \text{ pb})$				800
$\mu^+ \mu^-$			0.90	15
$e^+ e^-$				15

\* For final states involving K mesons the dominant inefficiency is from K/p separation below  $\sim 10 \text{ GeV/c}$

# Figure Captions

1. The  $P_T^2$  distribution for exclusively produced  $\pi^+\pi^-$  in E-87A.
2. The mass distribution for coherently produced  $\pi^+\pi^-$  in E-87A.
3. The inclusive  $\pi^+\pi^-$  mass distribution from E-87A.
4. The mass distribution for the lowest mass  $\pi^+\pi^-\pi^0$  combination within coherently produced  $\pi^+\pi^-\pi^+\pi^-\pi^0$  events in E-87A.
5. The energy dependence of  $d\sigma/dt$  at  $\theta = 0$  for the photo-production of  $\psi$  mesons. The fit curve is
 
$$\left. \frac{d\sigma}{dt} \right|_{\theta=0} = 66 (1-E_{th}/E)^{3.1} \text{ nb/GeV}^2 .$$
6. The photon energy spectra for various beams available at Fermilab:
  - a) broad band beam with  $6 \times 10^{12}$  400 GeV protons, large collimator hole, and 32 m of liquid  $D_2$ ,
  - b) tagged beam with  $6 \times 10^{12}$  450 GeV protons, a 20% radiator (untagged mode) and 100 GeV electrons,
  - c),d) same as b) with 150 GeV/200 GeV electrons.
7. The integrated photon spectra for the two Fermilab beams and the BEG beam at CERN. The CERN curve comes from the proposal SPSC/P 109.
8. The observed laboratory angle as a function of the center of mass angle for particles produced with  $m/P^* = 0, 0.5, \text{ and } 1$ .
9. The layout of the proposed detector shown in the non-bending view of the two magnets. The horizontal and vertical scales are the same.

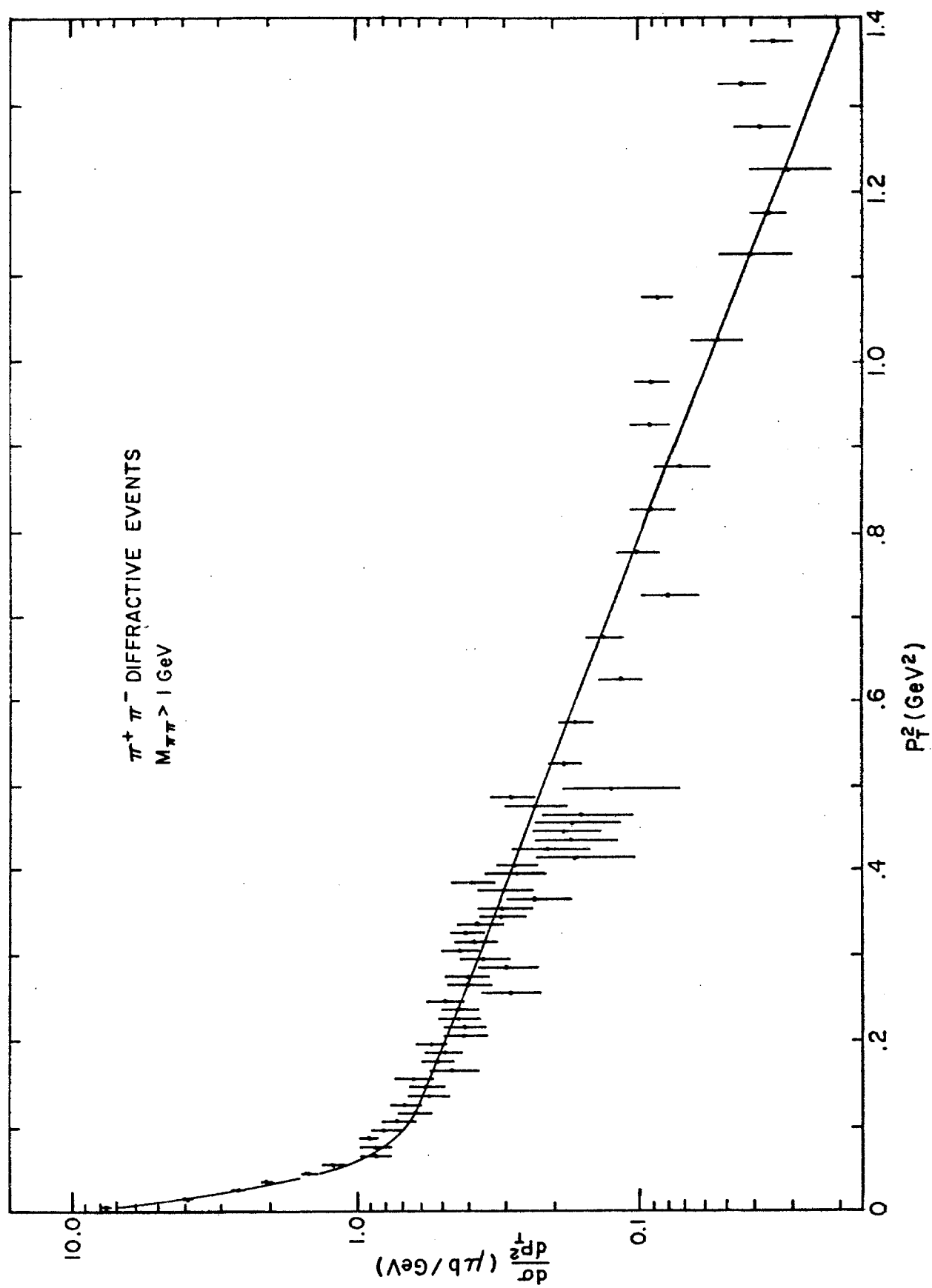


Fig. 1

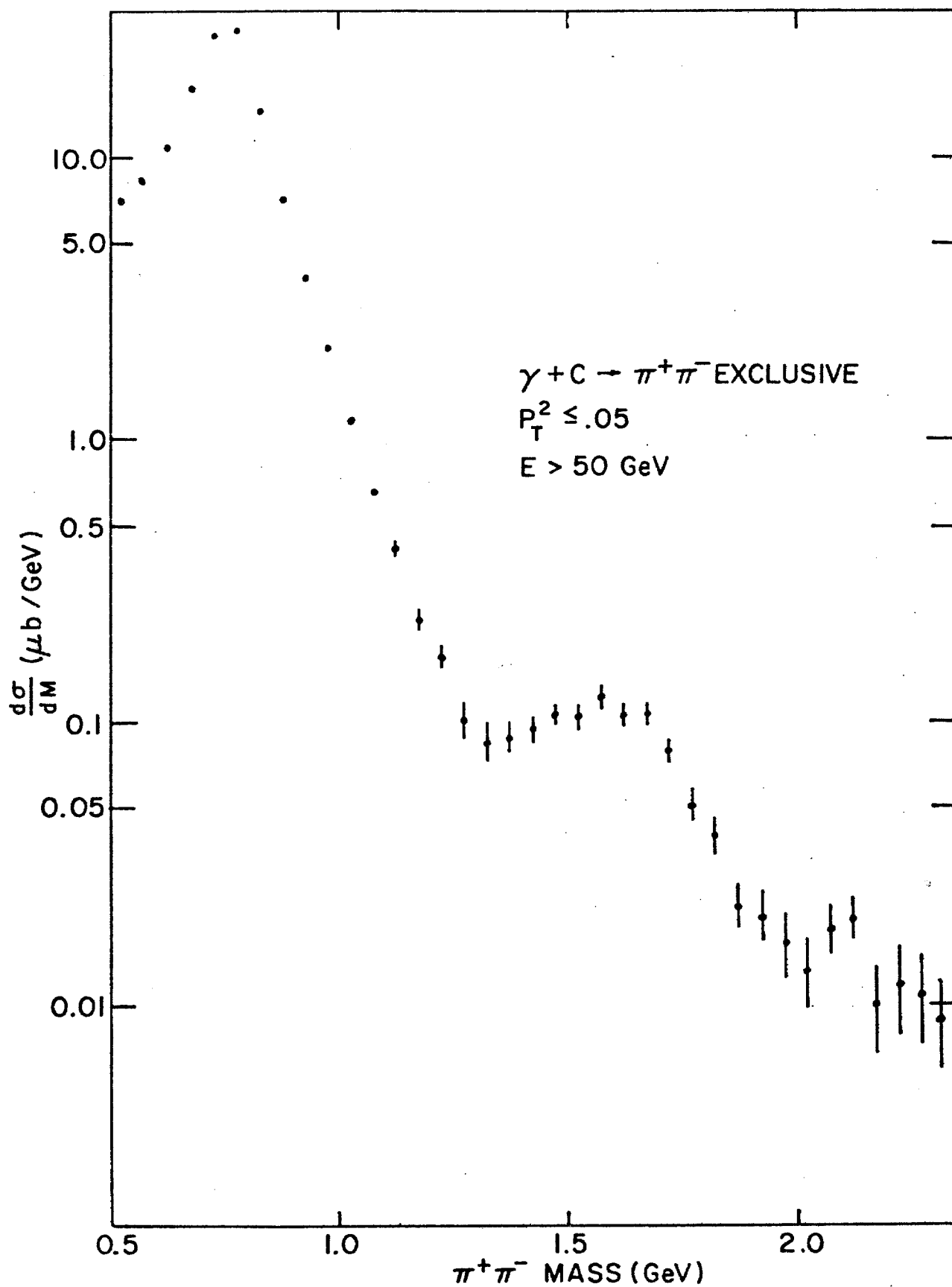


Fig. 2

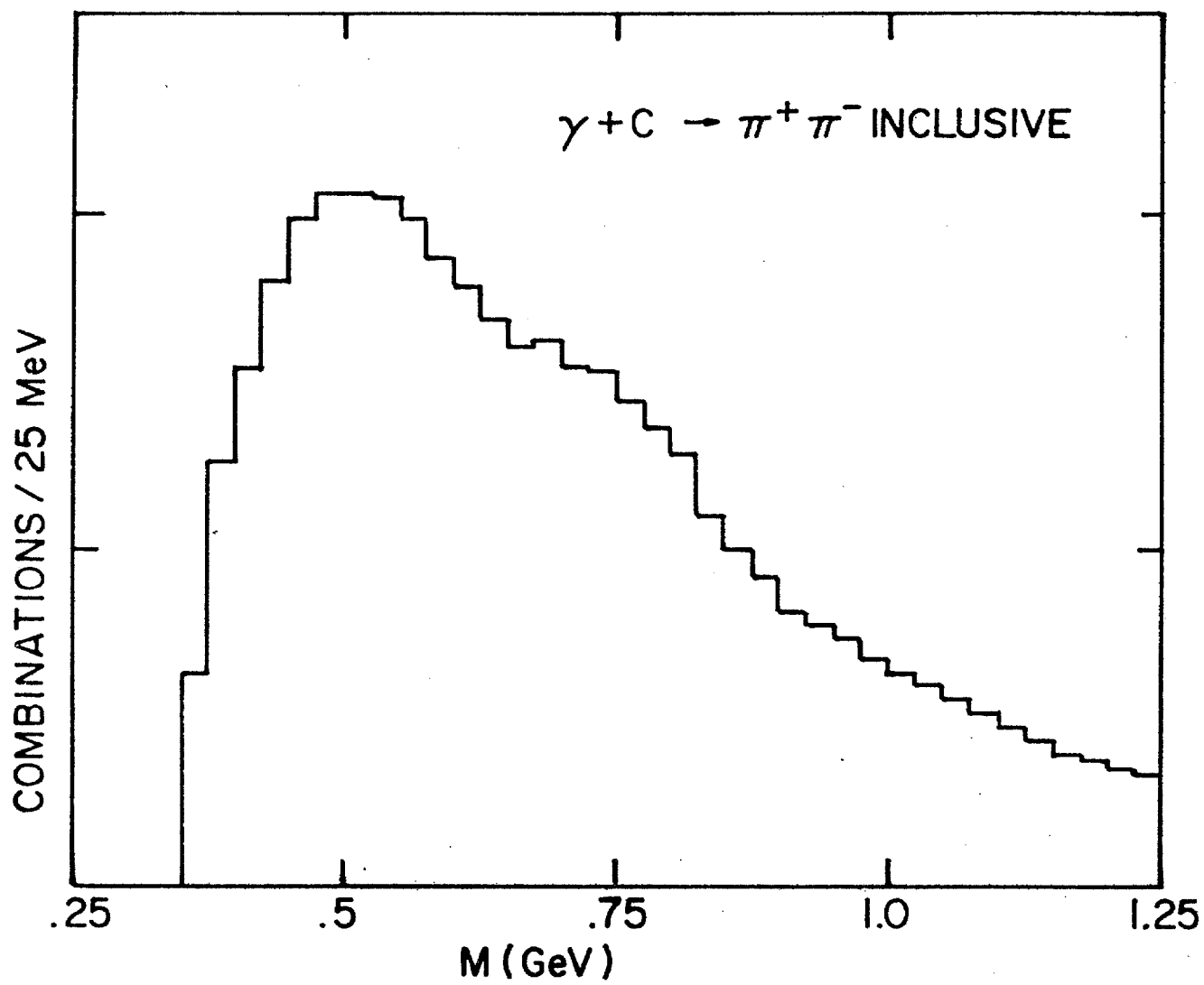


Fig. 3

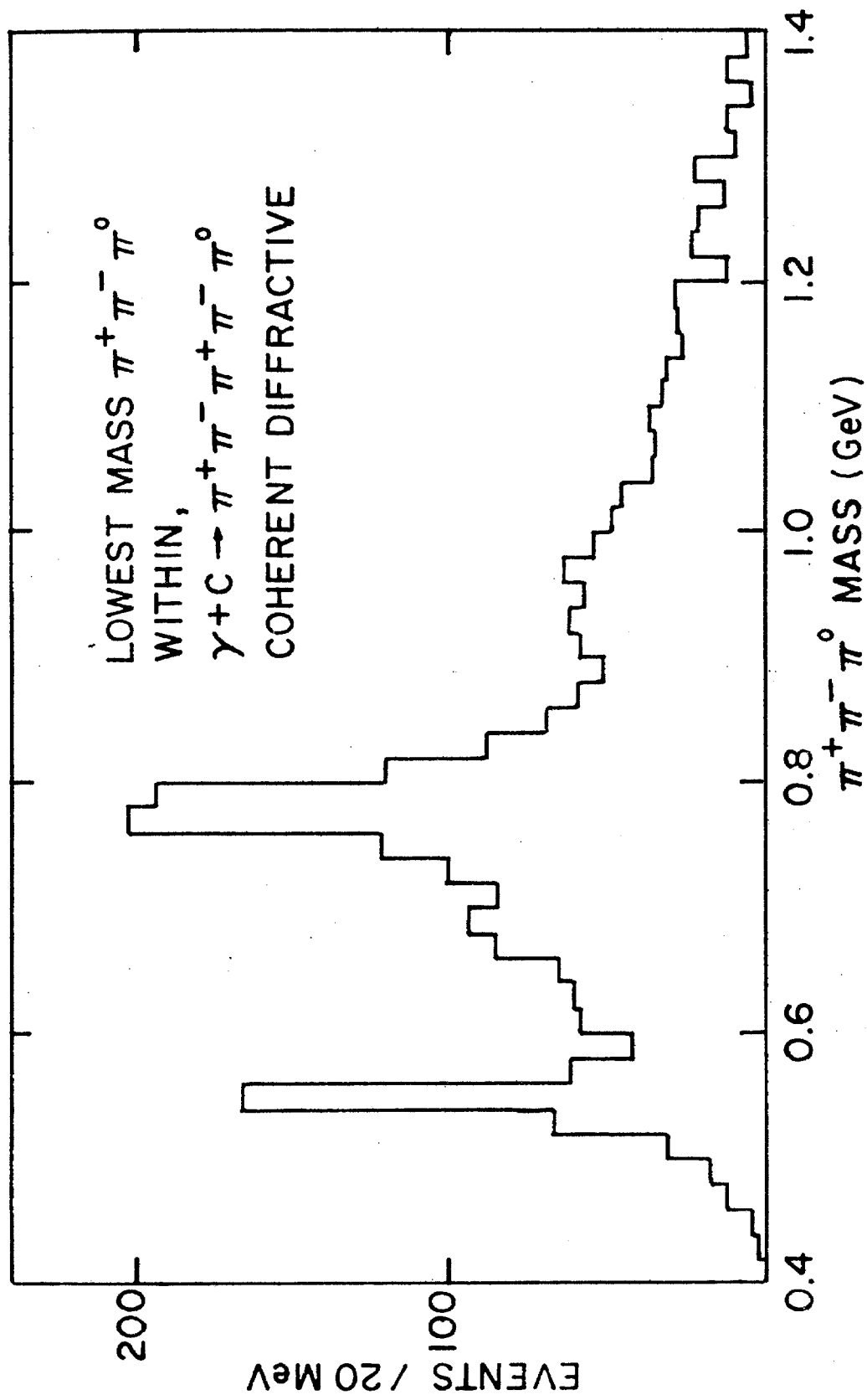


Fig. 4

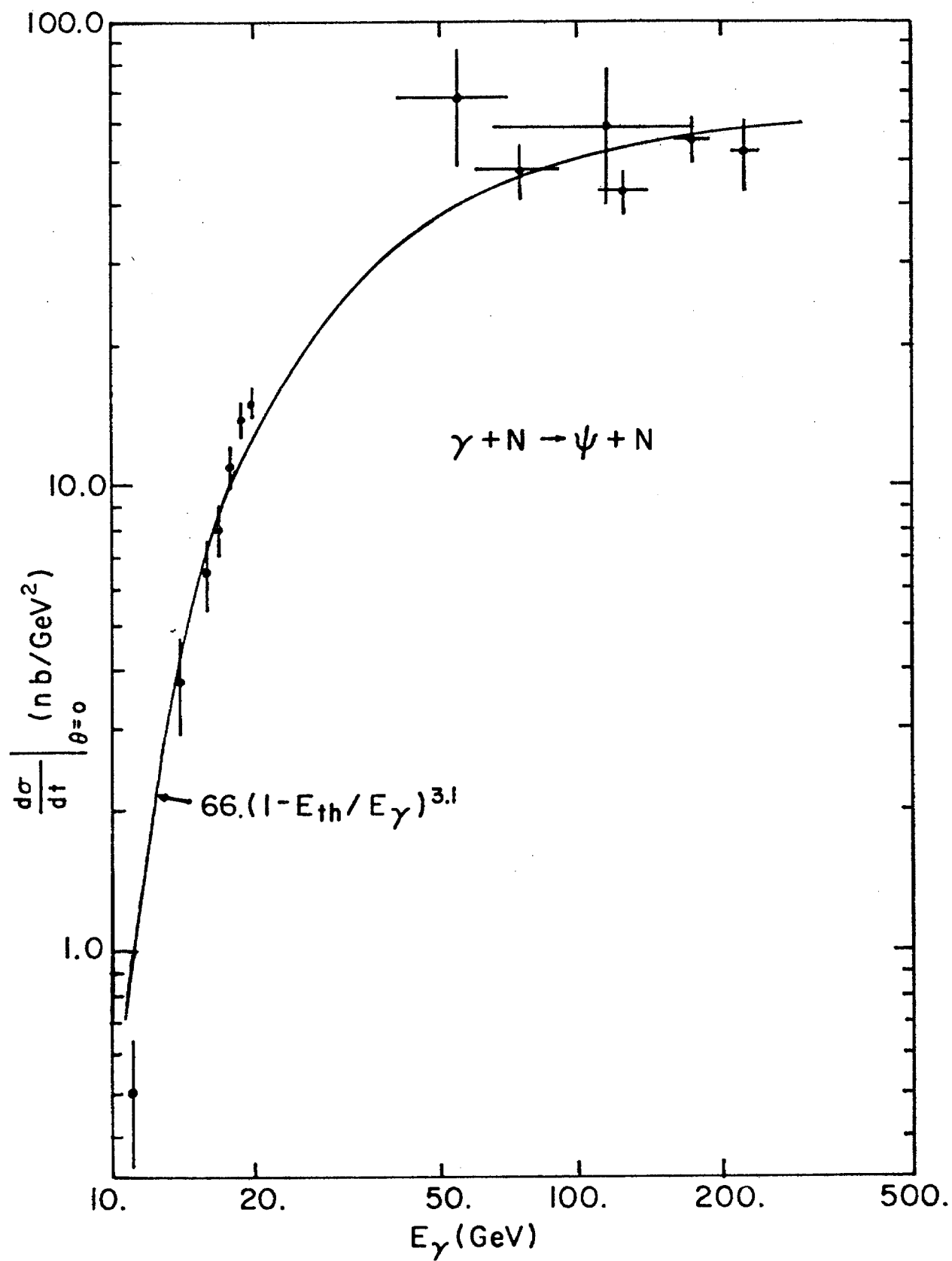


Fig. 5



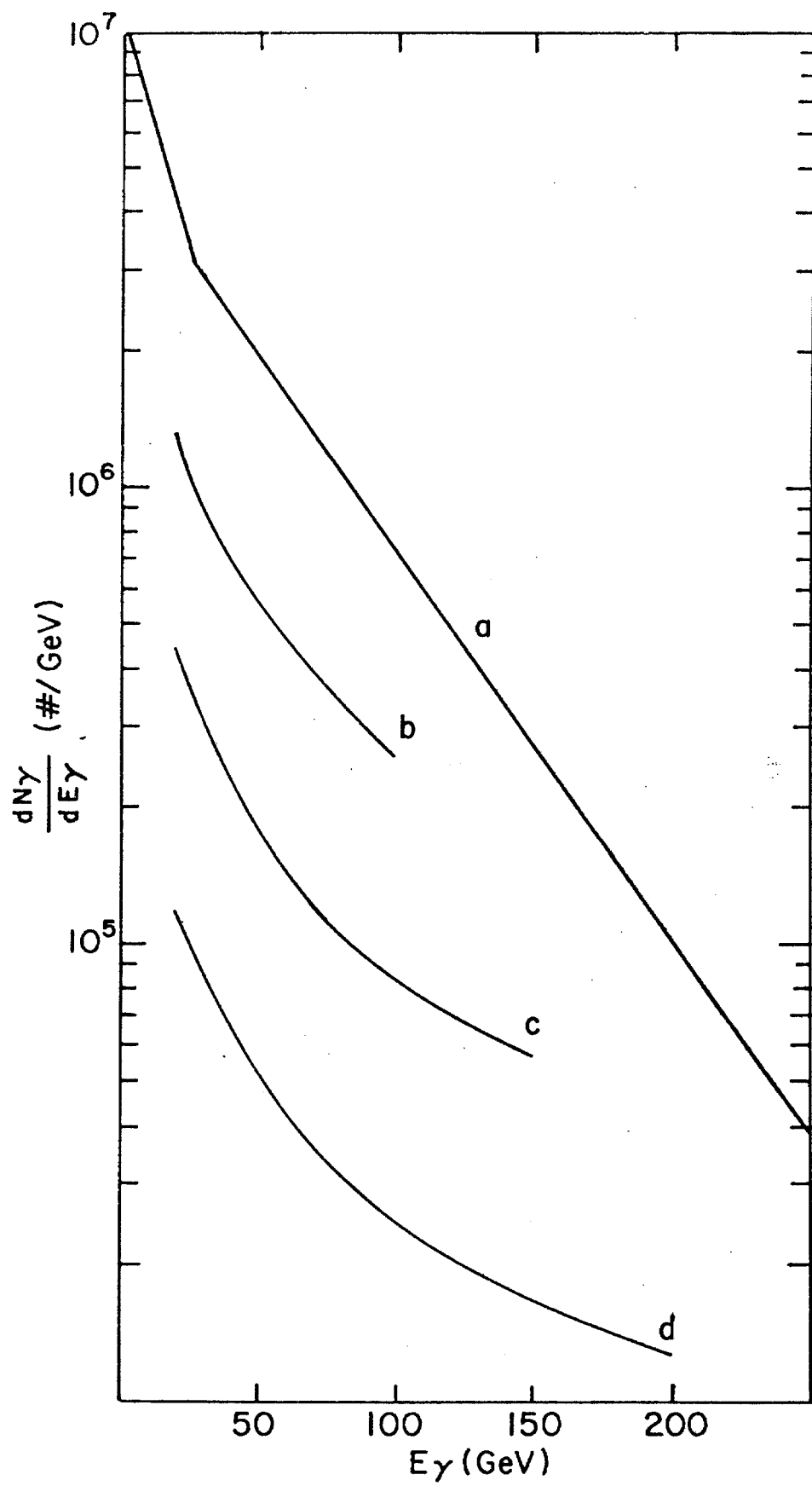


Fig. 6

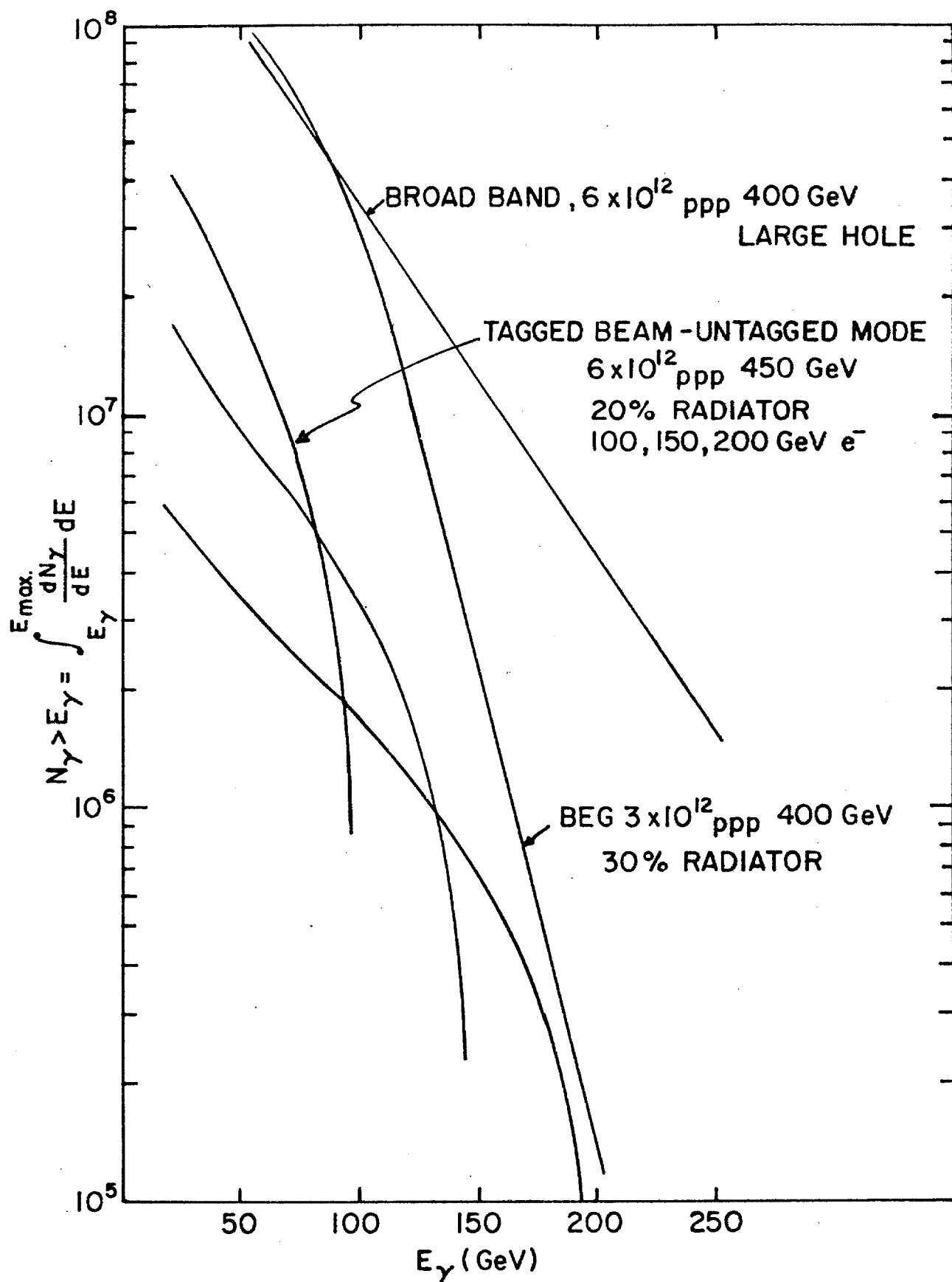


Fig. 7

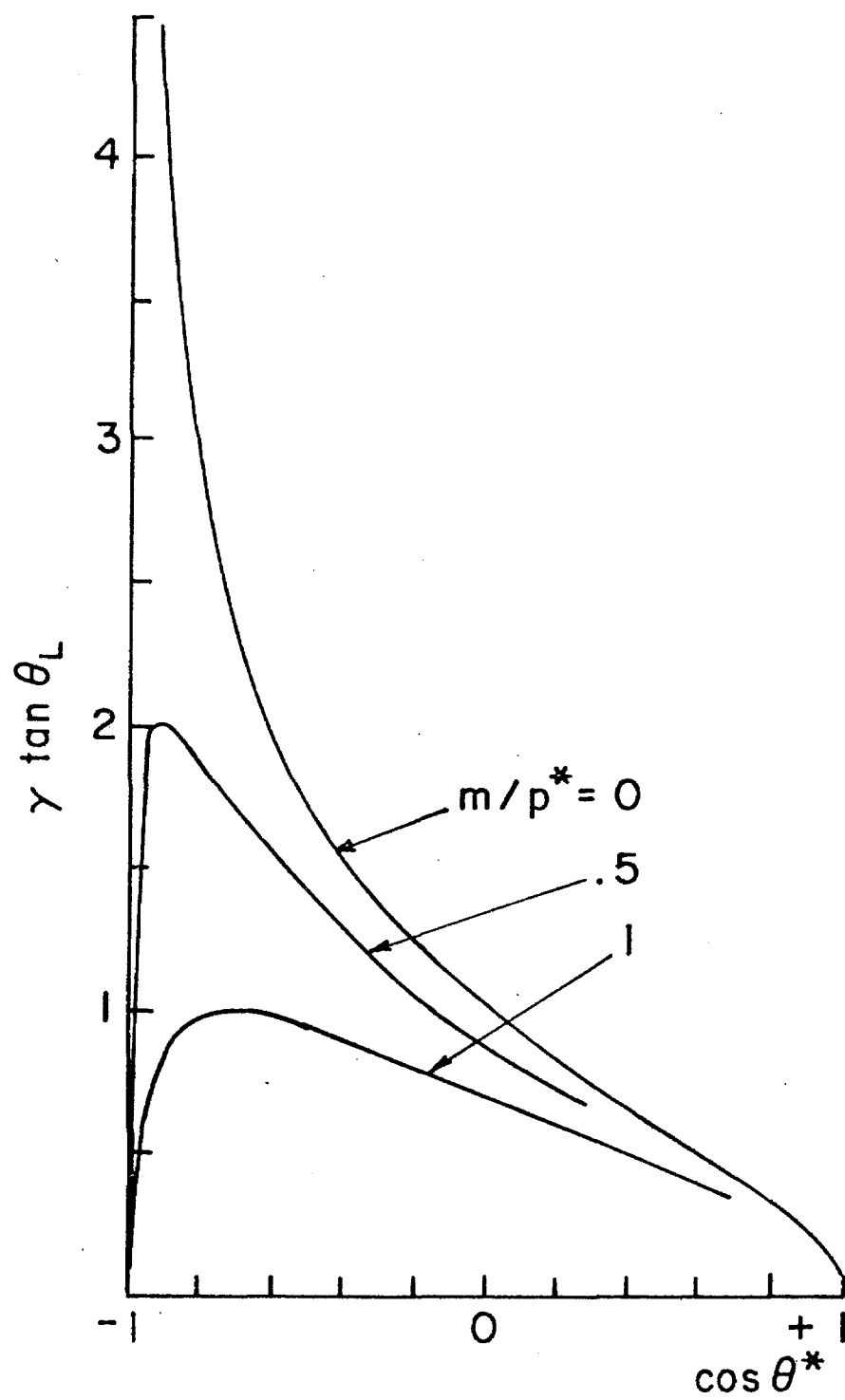


Fig. 8